

COMPARATIVE STUDY ON VARIOUS ARTIFICIAL MAGNETIC CONDUCTORS FOR LOW-PROFILE ANTENNA

J. R. Sohn, K. Y. Kim, and H.-S. Tae

School of Electrical Engineering and Computer Science
Kyungpook National University
Daegu 702-701, Korea

J.-H. Lee

Department of Radio Science and Communication Engineering
Hongik University
Seoul 121-791, Korea

Abstract—This paper investigated comparatively the characteristics of four types of artificial magnetic conductor (AMC) surface, including a mushroom-like (electromagnetic band gap) EBG, uniplanar compact EBG (UC-EBG), Peano curve, and Hilbert curve, as a ground plane for a low-profile antenna. The AMC surface structures are designed to have an in-phase reflection property for a plane wave of normal incidence in the vicinity of 2.45 GHz. The bandwidths of the in-phase reflection for the AMC surfaces and return losses, radiation patterns, and gains of the horizontal wire antennas on the AMC ground planes are all measured and compared with each other. The measured data show that all the AMC surfaces act as good ground planes for a low-profile antenna, yet the bandwidth and gain of the mushroom-like EBG structure are broader and larger, respectively, than those of the other structures.

1. INTRODUCTION

Artificial magnetic conductors (AMCs), also known as high-impedance surfaces [1], have received considerable attention in recent years [2–7]. An AMC is a type of electromagnetic band gap (EBG) material or artificially engineered material with a magnetic conductor surface for a

specified frequency band. AMC structures are typically realized based on periodic dielectric substrates and various metallization patterns [6–8], and several types of AMC ground planes have already been extensively studied [2–7].

AMC surfaces have two important and interesting properties that do not occur in nature and have led to a wide range of microwave circuit applications. First, AMC surfaces have a forbidden frequency band over which surface waves and currents cannot propagate [6], making them useful as ground planes and planar or waveguide type filters. For example, antenna ground planes that use AMC surfaces have good radiation patterns without unwanted ripples based on suppressing the surface wave propagation within the band gap frequency range [1]. Second, AMC surfaces have very high surface impedance within a specific limited frequency range, where the tangential magnetic field is small, even with a large electric field along the surface [6, 9]. Therefore, an AMC surface can have a reflection coefficient of +1 (in-phase reflection). Generally, the reflection phase is defined as the phase of the reflected electric field which is normalized to the phase of the incident electric field at the reflecting surface. It can be called in-phase (or out-of-phase) reflection, if the reflection phase is 0° (or not). In practice, the reflection phase of an AMC surface varies continuously from $+180^\circ$ to -180° relative to the frequency, and crosses zero at just one frequency (for one resonant mode). The useful bandwidth of an AMC is generally defined as $+90^\circ$ to -90° on either side of the central frequency. Thus, due to this unusual boundary condition, in contrast to the case of a conventional metal plane, an AMC surface can function as a new type of ground plane for low-profile wire antennas, which is desirable in many wireless communication systems. For example, even though a horizontal wire antenna is extremely close to an AMC surface, the current on the antenna and its image current on the ground plane are in-phase, rather than out-of phase, thereby strengthening the radiation.

Accordingly, this paper focuses on the antenna ground plane applications using the reflection phase feature of four types of AMC structure: a mushroom-like EBG [6], uniplanar compact EBG (UC-EBG) [7, 9], Peano curve [10], and Hilbert curve [4], as a ground plane for a low-profile antenna. All the AMC structures are designed using a full-wave simulation tool (CST Microwave Studio ver. 5.0). The reflection phases of the AMC surfaces and radiation characteristics, such as the radiation pattern, return loss, and gain of the horizontal wire antennas on the AMC ground planes, are measured using a standard horn antenna. For the comparison, the case of the conventional metal layer was also simulated and measured. All the

measured data are then analyzed and compared as regards using an AMC as a ground plane for a low-profile antenna.

2. FOUR TYPES OF AMC STRUCTURES

Figure 1 shows schematic diagrams of the four types of AMC structure, which were designed on substrates with a thickness t of 2.54 mm and relative permittivity ϵ_r of 6.0 (Rogers TMM6). The lattice in Fig. 1a consists of square metal patches connected to the continuous ground plane by pins, as in [6], while the lattice in Fig. 1b consists of square metal patches with four narrow connecting branches placed over the ground plane, as in [7]. As such, these two surface structures are periodically loaded with gap capacitances provided by the gaps between two neighboring metal patches and reactances provided by the shorting pins in Fig. 1a and narrow connecting branches in Fig. 1b.

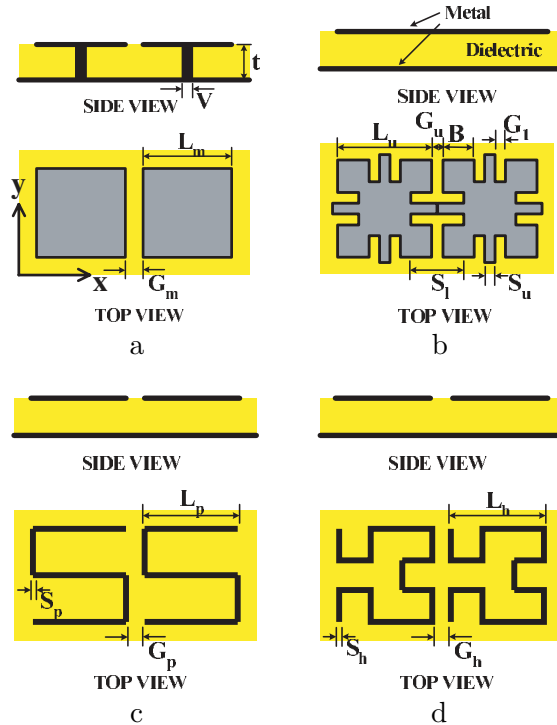


Figure 1. Schematics of artificial magnetic conductor (AMC) surfaces: a. Mushroom-like EBG, b. UC-EBG, c. first-order Peano curve, and d. second-order Hilbert curve.

Therefore, the two AMC surfaces in Figs. 1a and 1b are assigned impedance equal to that of a parallel LC circuit, derived by geometry, and have a high surface impedance at an LC resonance frequency. Parametric studies on LC resonance have already been well discussed in references [6–9].

Meanwhile, the Peano curve shown in Fig. 1c is a member of the family of curves known in mathematics literature as space-filling curves, which were introduced by Giuseppe Peano in 1890 [11], and the Hilbert curve in Fig. 1d, first proposed by David Hilbert in 1891, is also another type of space-filling curve. These curves map a one-dimensional interval, $(0, 1)$ into two-dimensional space, $(0, 1) \times (0, 1)$. As the iteration order number approaches infinity, the curves pass through every point in the 2-dimensional space in which they are contained, without intersecting themselves. These curves also provide resonant structures with a very small footprint when increasing the step order for the iterative filling of the 2-dimensional region. As the iteration order number of the curve increases, the curve maintains its footprint dimensions while the curve itself increases in length. Generally, because the compression rate of the Peano curve algorithm is relatively higher than that of the Hilbert curve algorithm, a Peano curve resonates at a lower fundamental resonant frequency than a comparable Hilbert curve of the same iteration order. This resonant property allows a surface with these curve inclusions to behave as an AMC surface. Thus, AMC surfaces with these curves have already been considered in antenna designs by several research groups, and the design characteristics of the AMCs are presented in reference [4, 10]. When considering a suitable bandwidth and unit cell size to compare the properties of the four types of AMC surface, a first-order Peano curve and second-order Hilbert curve were selected.

Using a full-wave simulation tool (CST Microwave Studio ver. 5.0) and some analytical models [6, 12], the four types of AMC surface were designed to include in-phase reflection for a normally incident plane wave on their surfaces at 2.45 GHz. The practical design specifications for each AMC surface are given in Table 1. Excluding the Peano and Hilbert curves, where the unit cell size decreases in proportion to the iteration order, the mushroom-like EBG structure was smaller than the UC-EBG structure, as shown Table 1. Figure 2 and Table 2 show the reflection phase diagrams and fractional bandwidths for the normal incident plane waves on the AMC surfaces, respectively. The reflection coefficient S_{11} for the AMC surfaces was measured using a standard horn antenna. The reflection phases were obtained by compensating the phases of the measured reflection coefficient for the phase shift by the distance between the AMC surface and the horn antenna. The

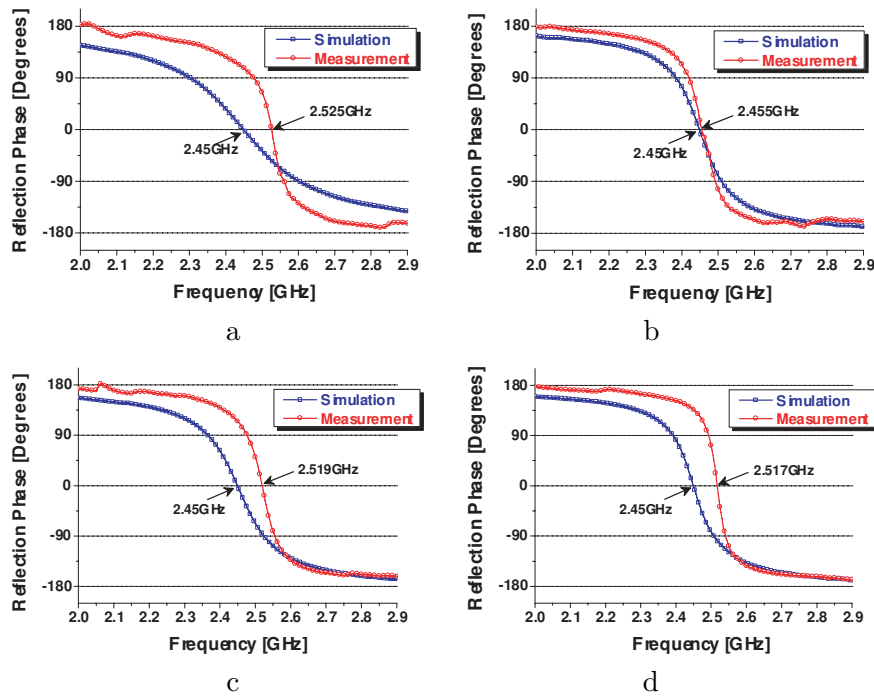


Figure 2. Measured and simulated results of reflection phase for AMC surfaces: a. Mushroom-like EBG, b. UC-EBG, c. first-order Peano curve, and d. second-order Hilbert curve.

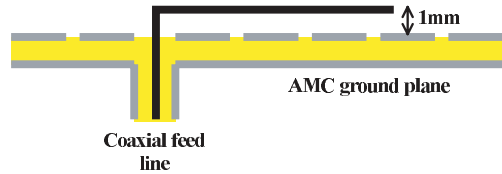
simulated and measured reflection phases of the conventional metal layer are 180 as have been mentioned previously. Because it is well known problem in electromagnetic wave theory, we did not include this result in Figure 2. All the AMC structures were fabricated on a TMM6 substrate, 150 mm \times 190 mm in size. As shown in Fig. 2, the measured reflection phases for all the AMC surfaces varied continuously from $+180^\circ$ to -180° relative to the frequency, and were equal to zero degrees near 2.45 GHz, meaning that all the AMCs were successfully realized. All the full-wave simulations showed a close agreement within an error of 3%, which may have been caused by the finite substrates and fabrication errors. From the bandwidths listed in Table 2, the mushroom-like EBG had the widest bandwidth compared to the other structures.

Table 1. Design specifications for each AMC unit cell structure.

| AMC Type | Design Specification [mm] |
|--------------------------|---|
| Mushroom-like EBG | Lm=18.2, Gm=1, V=1 |
| UC-EBG | Lu=20, B=7.5, Su=0.6, Sl=11.3, G1=2.2, Gu=1 |
| Peano curve of order 1 | Lp=19, Sp=1, Gp=1.5 |
| Hilbert curve of order 2 | Lh=11.4, Sh=0.7, Gp=1.5 |

Table 2. Simulated and measured bandwidths of AMC surfaces. Here, $f_{\phi=0}$ is the frequency point with a reflection phase of 0° and Δf is defined as $\pm 90^\circ$ crossings for the reflection phase.

| AMC Type | Bandwidth ($\Delta f / f_{\phi=0}$) | |
|--------------------------|---------------------------------------|-------------|
| | Simulation | Measurement |
| Mushroom-like EBG | 12.08 % | 3.46 % |
| UC-EBG | 4.88 % | 2.95 % |
| Peano curve of order 1 | 6.30 % | 3.14 % |
| Hilbert curve of order 2 | 4.69 % | 1.93 % |

**Figure 3.** Schematic illustration of horizontal wire antenna on AMC ground plane.

3. HORIZONTAL WIRE ANTENNA ON AMC GROUND PLANE

Generally, a horizontal wire antenna radiates very poorly on a conventional metal ground plane, as the image currents cancel the currents in the antenna. However, the same wire antenna on an AMC surface, as shown in Fig. 3, performs well due to the in-phase reflection property of the AMC surface. In Fig. 3, the coaxial-fed wire antenna is bent over so that it lies parallel to the ground plane and 1mm above the four types of AMC surface. The length of the wire antenna was tuned to near half the wavelength for a small return loss. Figure 4 shows photographs of the horizontal wire antennas built on the AMC

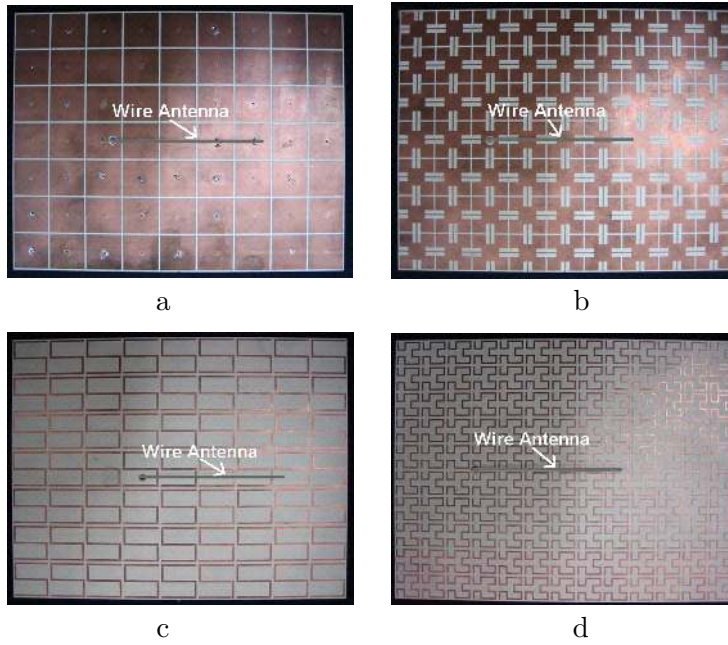


Figure 4. Photographs of horizontal wire antenna on AMC ground planes: a. Mushroom-like EBG, b. UC-EBG, c. first-order Peano curve, and d. second-order Hilbert curve.

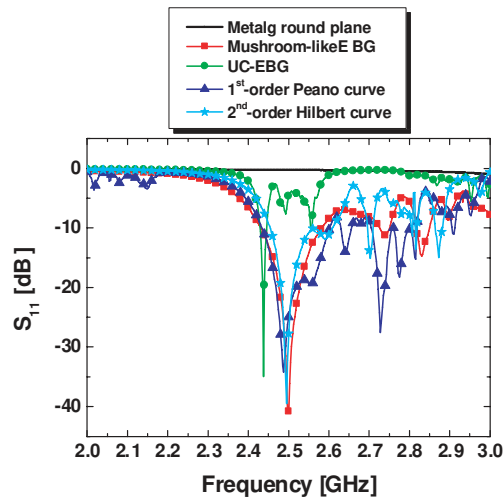


Figure 5. Measured return losses of horizontal wire antenna on AMC ground planes.

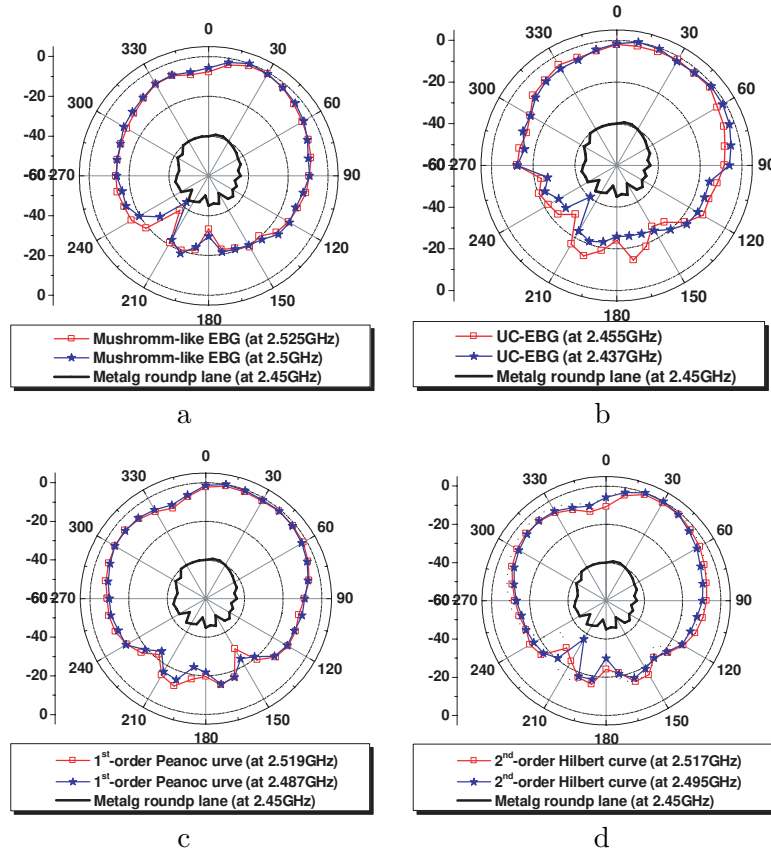


Figure 6. Measured E-plane radiation patterns of horizontal wire antenna on AMC ground planes; a. Mushroom-like EBG, b. UC-EBG, c. first-order Peano curve, and d. second-order Hilbert curve.

ground planes that were realized using printed circuit board technology using the design specifications in Table 1.

Figure 5 shows that the wire antennas on all the ground planes were well matched with below -20 dB return losses, meaning that most of the power radiated through the wire antennas, although the wire antenna on the conventional metal ground plane radiated very poorly. Figure 6 shows the E-plane radiation patterns, measured using a standard horn antenna. The radiation patterns were measured at two frequency points: the reflection phase of zero degrees in Fig. 2 and the smallest return loss (S_{11}) in Fig. 5. The frequency with the 0° reflection phase was not consistent with the input-match frequency,

Table 3. Measured gain of horizontal wire antenna on AMC ground planes. The gains were measured at the frequency points with the smallest S_{11} value.

| AMC Type | Antenna Gain [dBi] |
|--------------------------|--------------------|
| Mushroom-like EBG | 9.1 |
| UC-EBG | 7.69 |
| Peano curve of order 1 | 8.27 |
| Hilbert curve of order 2 | 8.1 |

as for the low-profile antennas on the AMC surfaces, a normally incident plane wave was not applied to the AMC surfaces. Namely, more complicated interactions occurred between the antennas and the AMC surfaces. This property has also been confirmed in another low-profile antenna application [2]. The wire antennas on the AMC ground planes radiated very well in contrast to those on the conventional metal grounds, and a better radiation pattern was obtained at the input-match frequency. Table 3 shows the antenna gain measured by using the gain comparison method [13], confirming that when using an AMC ground plane, the wire antenna had a higher gain than any other type of wire antenna because of the in-phase reflection and surface wave suppressing properties of the AMC ground planes. Thus, from the results in Table 3, the mushroom-like EBG structure was found to be most suitable for high-gain antenna applications.

4. CONCLUSION

AMC structures, including a mushroom-like EBG, UC-EBG, 1st-order Peano curve, and 2nd-order Hilbert curve, were comparatively investigated using a full-wave simulation and experiment. The AMC structures were all designed to have an in-phase reflection property for a plane wave of normal incidence in the vicinity of 2.45 GHz. The measured bandwidth of the reflection phase for the mushroom-like EBG surface was broader than those for all the other surfaces. To use the AMC structures as a ground plane for low-profile antennas, horizontal wire antennas were realized on the AMC surfaces. The wire antennas on the AMC ground planes were all well matched with below -20 dB return losses. The frequency point with the smallest return loss and frequency for the 0° reflection phase were not necessarily consistent due to complicated interactions between the antenna and the AMC surface. The radiation patterns and wire antenna gains for the various AMC ground planes were measured and compared with each other. All

the AMC ground planes offered good radiation patterns and high gains. The performance comparison results might be useful in providing some design guidelines using these AMC surfaces or ideas in choosing proper AMC surfaces for specific applications. In particular, the mushroom-like EBG surface had an advantage in the bandwidth and gain over the other AMC surfaces. As a result, some AMC design guidelines are suggested for low-profile antenna applications.

ACKNOWLEDGMENT

This work was supported by Korea Research Foundation Grant (KRF-2003-041-D00465).

REFERENCES

1. Sievenpiper, D., "High-impedance electromagnetic surfaces," Ph.D. Thesis, University of California, Los Angeles, 1999.
2. Yang, F. and Y. Rahmat-Samii, "Reflection phase characterizations of the EBG ground plane for low profile wire antenna applications," *IEEE Trans. Antennas Propag.*, Vol. 51, No. 10, 2691–2703, 2003.
3. Zhang, Y., J. von Hagen, and W. Wiesbeck, "Patch array as artificial magnetic conductors for antenna gain improvement," *Microw. Opt. Technol. Lett.*, Vol. 35, No. 3, 172–175, 2002.
4. McVay, J., N. Engheta, and A. Hoorfar, "High impedance metamaterial surfaces using Hilbert-curve inclusions," *IEEE Microw. Wire. Comp. Lett.*, Vol. 14, No. 3, 130–132, 2004.
5. Feresidis, A. P., S. Wang, and J. C. Vardaxoglou, "Artificial magnetic conductor surfaces and their application to low-profile high-gain planar antennas," *IEEE Trans. Antennas Propag.*, Vol. 53, No. 1, 209–215, 2005.
6. Sievenpiper, D., L. Zhang, R. F. J. Broas, N. G. Alexopolous, and E. Yablonovitch, "High-impedance electromagnetic surfaces with a forbidden frequency band," *IEEE Trans. Microwave Theory Tech.*, Vol. 47, No. 11 2059–2074, 1999.
7. Yang, F. R., K. P. Ma, Y. Qian, and T. Itoh, "A uniplanar compact photonic-bandgap (UC-PBG) structure and its applications for microwave circuit," *IEEE Trans. Microwave Theory Tech.*, Vol. 47, No. 8, 1509–1514, 1999.
8. Barlevy, A. S. and Y. Rahmat-Samii, "Characterization of electromagnetic band-gaps composed of multiple periodic tripods

- with interconnecting vias: Concept, analysis, and design," *IEEE Trans. Antennas Propag.*, Vol. 49, No. 3, 343–353, 2001.
9. Yang, F. R., K. P. Ma, Y. Qian, and T. Itoh, "A novel TEM waveguide using uniplanar compact photonic-bandgap (UC-PBG) structure," *IEEE Trans. Microwave Theory Tech.*, Vol. 47, No. 11, 2092–2098, 1999.
 10. McVay, J., A. Hoorfar, and N. Engheta, "Small dipole-antenna near Peano high-impedance surfaces," *IEEE AP-S Int. Symp.*, Vol. 1, 305–308, 2004.
 11. Sagan, H., *Space-Filling Curves*, Springer-Verlag, New York, 1994.
 12. Rahman, M. and M. A. Stuchly, "Transmission line-periodic circuit representation of planar microwave photonic bandgap structures," *Microw. Opt. Tech. Lett.*, Vol. 30, No. 1, 15–19, 2001.
 13. Stutzman, W. L. and G. A. Thiele, *Antenna Theory and Design*, 2nd ed., John Wiley & Sons, Inc., New York, 1998.